10th IMEKO TC14 Symposium on
Laser Metrology for Precision Measurement and Inspection in Industry
Braunschweig, GERMANY, 2011, September 12-14

Determination of Stochastic Phase Shifts in Random Phase Shift Interferometric Testing of Spherical Surfaces

Hagen Broistedt, **Rainer Tutsch**, Institut für Produktionsmesstechnik (IPROM) Technische Universität Braunschweig, Braunschweig

Abstract:
To measure the topography of a surface by conventional phase shifting interferometers, exactly known phase shifts between reference and test surface are required. To keep the phase shifts stable during measurement, the interferometers are mounted on vibration isolation tables. To overcome the necessity of expensive vibration isolation equipment, in [1] a low cost interferometer for plane surfaces had been presented that copes with vibration, and makes use of the vibrations to create phase shifts during the measurement. This article describes the extension of this approach to the measurement of spherical surfaces in the presence of vibrations.

Description of the random phase shift interferometer
In conventional phase shift interferometers only one sensor with high spatial resolution, usually consisting of a CCD or CMOS image sensor, is necessary. In case of the presented random phase shift interferometer a second detector with high temporal resolution had to be integrated. The experimental arrangement is shown in the Fig 1. The measurement system is a modified Fizeau-Interferometer. A He-Ne laser beam of 632.8 nm wavelength is directed to the spatial filter SF, using the mirrors M1 and M2 and collimated with the collimating lens L1 to the test and reference round plates T and R.
The reflected wavefronts from the test and reference surfaces are both partially reflected by the beam-splitter BS-1 and traced through a pinhole aperture. Further using the beam-splitter BS-2 the interference field is divided and guided to the two different detector systems. The reflected part is projected onto a CCD sensor array of the camera (high spatial but low temporal resolution detector). The transmitted part is collimated by the collimating lens L2 and hits three photodiodes (high temporal but low spatial resolution detector system).

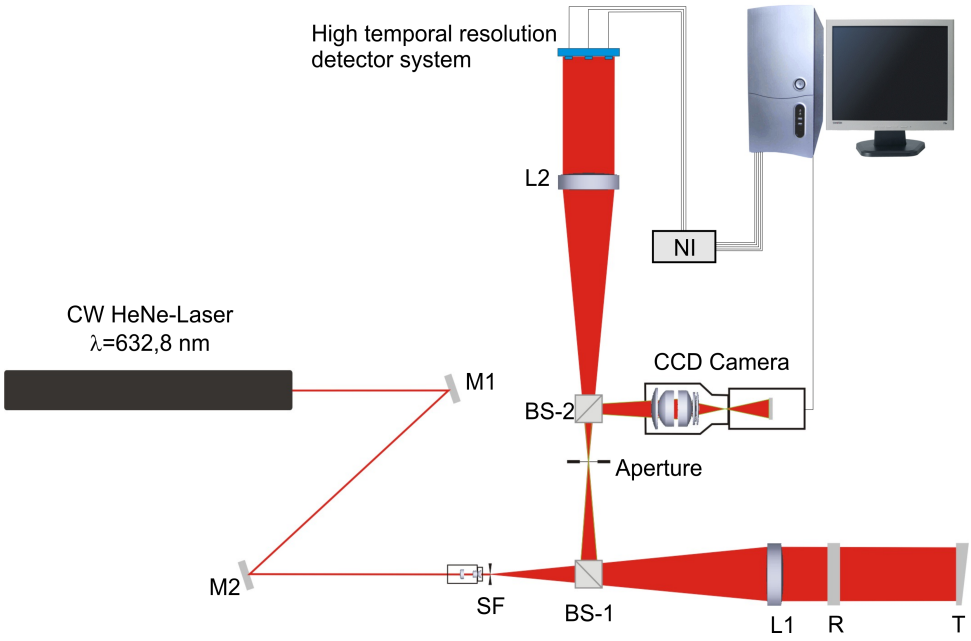

Fig. 1: Experimental setup for the random phase shift Fizeau-Interferometer for plane surfaces

The functional principle is as follows: the CCD camera records a few interferogram images with random phase shifts due to the influence of the vibrations. The camera runs at 25 fps with an exposure time of only 11 µs, which is short enough to freeze mechanical vibrations. While the camera grabs several interferograms, the high temporal resolution detector system continuously records the light intensities which occur at three locations in the interference field aperture (Fig. 2).

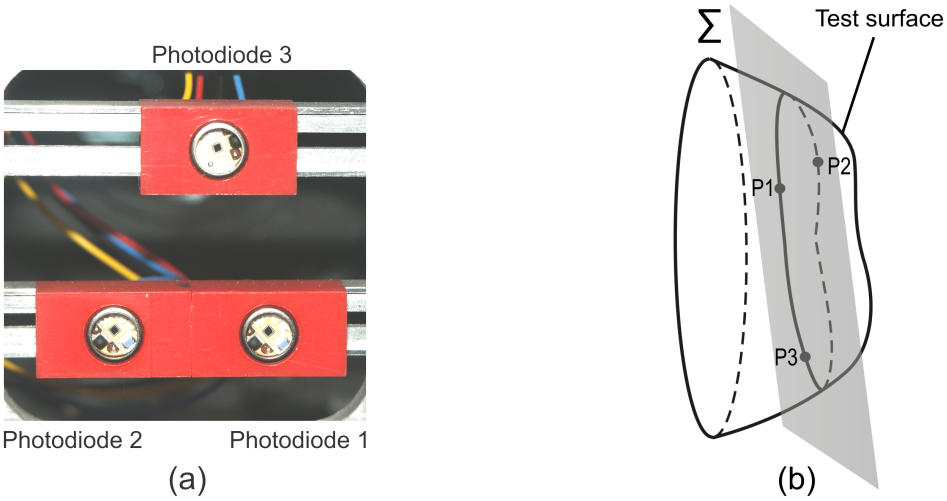

Fig. 2: The high temporal resolution detector system consisting of three photodiodes (a). The three corresponding non-collinear measurement points P1, P2 and P3 on the test surface which define the oscillating plane Σ (b)

Due to the knowledge of the position of the photodiodes and the measured relative movement between reference and test plate in these points, it is possible to calculate the movement of the entire plane Σ. The plane equation for Σ enables the evaluation of the random phase shift in every image point of the corresponding interference image taken by the CCD Camera.
Dealing with random phase shifts, a four step random phase shift algorithm was developed to calculate the test surface topography from the interferograms.

Modified approach for the random phase measurement of spherical surfaces

The position and orientation of a flat surface is determined by three non-collinear points. As well it is possible to define the location of a sphere, by known coordinates of four different points of the spherical surface that must not lie on one circle.
A sphere position is defined by its centre point. The centre point can be calculated with the sphere equation:

$$(x_i - x_m)^2 + (y_i - y_m)^2 + (z_i - z_m)^2 - R^2 = 0 \quad (1)$$

where x_i, y_i, z_i are the coordinates of a point P_i lying on the spherical surface and x_m, y_m, z_m are the coordinates for the centre point M of the sphere with the radius R. To calculate a sphere movement, by the centre point movement, one needs to know at least three points and the radius of the sphere, or four points without knowing the radius. In this work four photodiodes were used for the calculation. A 2D section drawing of a sphere Sp1, which was moved by Δz in z-direction to the position Sp2, is shown in Fig. 2. To solve the sphere equation, the first point P1 on the shifted sphere has to be calculated. This is possible by measuring the optical path difference dOPD1 between Sp1 and Sp2 along a fixed axis A1 with angle α_1. Within the xz-plane (y=0) the x and z coordinates of the sampling points are evaluated from:

$$z_i = (R + dOPD_i) \cdot \cos(\alpha_i) \quad ; \quad i = 1,...4 \quad (2)$$

$$x_i = (R + dOPD_i) \cdot \sin(\alpha_i) \quad ; \quad i = 1,...4 \quad (3)$$

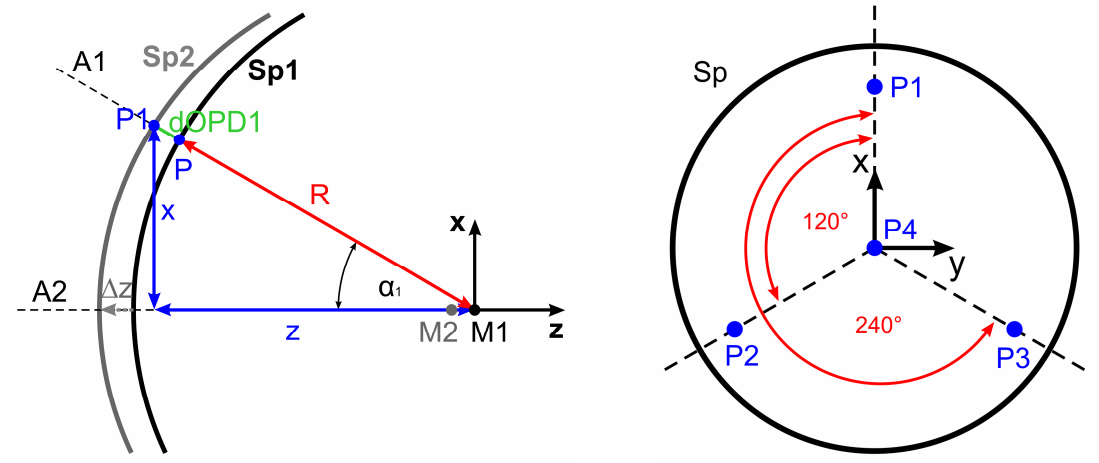

(a) (b)

Fig. 3: Schematic diagram of a 2D section drawing of a sphere Sp1 that is moved into the position Sp2 (a). Distribution of measured points on the sphere in the xy-plane (b).

The other two points P2 and P3 on Sp2 are observed in a similar way. To get a good distribution of the calculated points on the sphere surface, P2 is measured in a rotated position by ω_2 = 120° around the z-axis and P3 is rotated by ω_3 = 240° (Fig. 3 (b)). Coordinates of the points P2 and P3 are calculated in rotated coordinate systems (with rotation angle around the z-axis ω_2 and ω_3 respectively). The equation for a backward rotation from the point P'_i in the rotated coordinate system to a point P_i in the fixed coordinate system is [2]:

$$P_i = R_\omega \cdot P'_i \quad ; \quad \begin{pmatrix} x_i \\ y_i \\ z_i \end{pmatrix} = \begin{pmatrix} \cos\omega_i & -\sin\omega_i & 0 \\ \sin\omega_i & \cos\omega_i & 0 \\ 0 & 0 & 1 \end{pmatrix} \cdot \begin{pmatrix} x'_i \\ y'_i \\ z'_i \end{pmatrix} \qquad (4)$$

where R_ω is the rotation matrix around the z-axis with angle ω. x_i, y_i, z_i are the coordinates in the fixed coordinate system and x'_i, y'_i, z'_i are the coordinates in the rotated coordinate system. For the evaluation of (x'_2, y'_2, z'_2) and (x'_3, y'_3, z'_3), the same equations (2) and (3) can be used, just by changing the corresponding $dOPD_i$ and angle α_i. P4 is positioned directly on the z-axis ($y_4 = x_4 = 0$). Using four known points on the sphere, the centre point M2 can be calculated. Substituting equation (1), any point of the sphere can be determined.

Setup for the Simulation

In case of spherical surfaces measurement, the experimental setup in Fig. 1 has to be changed. Instead of a plane test and reference surface T and R, a spherical test surface combined with a measurement objective has to be applied. The measurement objective

creates the reference wavefront and transforms the incoming plane wavefront to a spherical one. The test surface is brought to a position where it fits the wavefront. Additionally a fourth photodiode has to be included in the temporal detector system to measure the relative phase shift in four points.

A setup of this approach without a simplified measurement objective was simulated with the optic design software Zemax (Fig. 4).

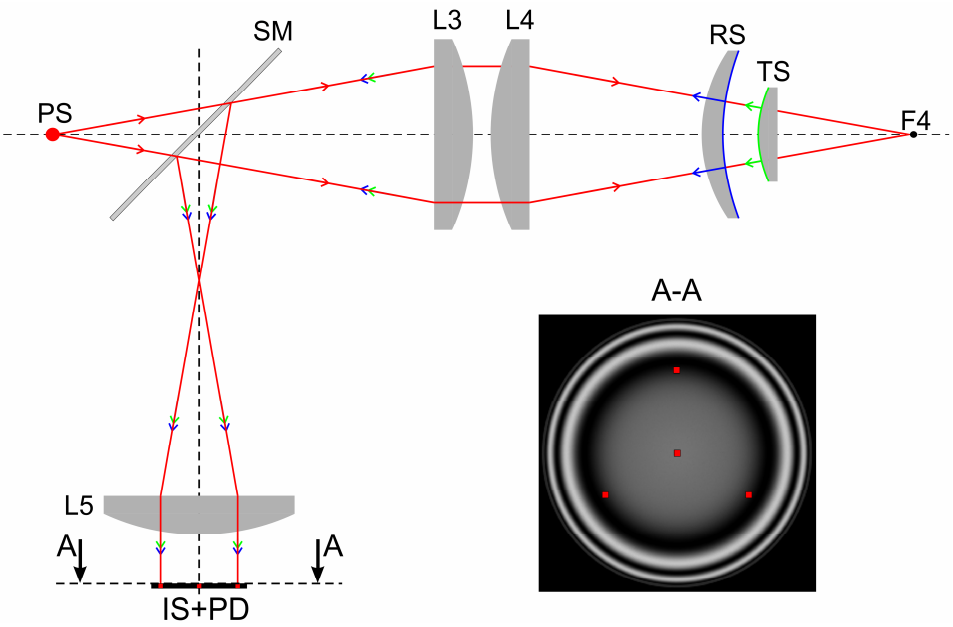

Fig. 4: Schematic view of the setup in the Zemax-simulation to measure the movement of a reference sphere relative to the test sphere.

The light from an ideal coherent point source PS of wavelength 632.8 nm is collimated by the collimation lens L3. The collimated beam goes through a second collimation lens L4 which forms a spherical wavefront. The center point of the wavefront lies in the focal point F_4 of L4. The reference surface (RS) and the test surface (TS), realized by two additional lenses, are located concentrically to the point F_4. RS belongs to a meniscus lens, which spherical back surface reflects the reference wavefront. The refraction of the meniscus lens in Zemax is neglected, by setting the refractive index to 1, so there is no additional deformation of the reflected wavefronts by this lens. TS is the convex spherical surface with radius 77.52 mm of a plano-spherical lens, which reflects the test wavefront. The reflections from the plane back surface also were neglected in Zemax. Furthermore reference and test wavefront are reflected by a semitransparent mirror SM to a third collimation lens L5, which images the interfering test and reference wavefront on an image sensor IS. This image sensor is the high spatial resolution sensor and has a pixel resolution 1000x1000. Additionally four small

sensors (PD) that represent the photodiodes, are placed in the plane of the image sensor, arranged like in Fig. 3(b). A calculated interference image of the sphere surface without shift is also shown in the section drawing A-A. The red squares are the simulated photodiodes with 1 mm^2 sensitive area. In case of perfectly equal test and reference wavefront, the intensity on the image sensor would be equal. But due to the aberrations of the collimation lenses, obviously both wavefronts are deformed towards the edge of the aperture. So the photodiodes are placed at the rim of the almost homogeneous intensity area in the middle, so this effect shouldn't have significant influence on the measurement. The angle α_n in equation (2) and (3) is known from the position of the photodiodes and amounts α_1 =15°, α_2 =15°, α_3 =15°, α_4 =0°.

Measurement of the movement of the sphere

The continuously changing interference fringes caused by the relative shift between reference and test surface are measured by the photodiodes. To fulfil the sampling theorem, the frequency has to be large enough that the shift between two adjacent samples is smaller than a quarter of the wave length. In the simulation it is made a realistic assumption of a maximum shift of 10 wavelength like it was observed in the experiments with the plane surfaces [3]. 140 interferograms were simulated for equidistant steps, resulting in 7 samples per period of the oscillating intensity signal. For the x direction a sine fit through the taken measuring points seemed to be sufficient to recover the continuous interference signal (Fig. 5). One parameter from the sine fit-function gave the wavelength of the fit-function. The z-axis shows the movement of the sphere but not the measured distance of the photodiode, which have to be calculated. After unwrapping the signal based on to the knowledge of the sine-fit wavelength, the real measured distance dOPD can be calculated from the known applied light wavelength. In this way $dOPD_i$ is calculated for every photodiode. With the known radius *R* and equation (2), (3),(4) the corresponding points P1, P2, P3, P4 on the shifted sphere are evaluated. With known radius of the sphere, there are four equations with three unknowns and the equation system is overdetermined. The least square method was chosen to solve the equation system.

For the movement of the sphere in z-direction the deviation between real sphere position (x = 0 µm , y = 0 µm, z = 6.283 µm) and the calculated sphere position amounts x = -3,6011E-02 nm, y = -7,5756E-02 nm, z = 3,39198 nm.

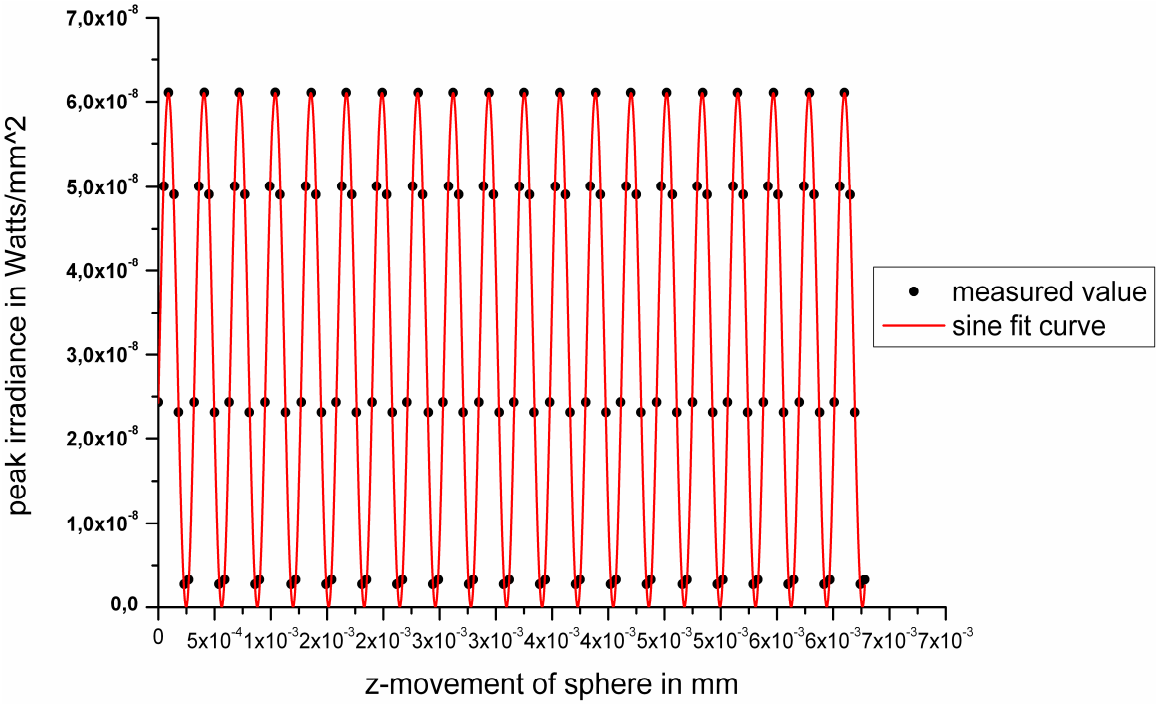

Fig. 5: Measured intensities for a photodiode during the movement of the reference sphere in z-direction about 10 waves (in black). The red curve shows the sine fit calculated through the measuring points.

Conclusion

The paper presents an approach to modify a random phase shift interferometer for plane surfaces to the measurement of spherical surfaces. Therefore the stochastic relative phase shift between reference and test sphere has to be determined. It is shown how to calculate the movement of the test surface relative to the reference surface with a sphere equation by the measurement of four points on the test sphere. This algorithm is verified in a simulation of a test setup.

[1] Doloca, R.; Broistedt, H.; Tutsch, R.: *Phase-shift Fizeau interferometer in presence of vibration.* In: Novak, E. L.; Osten, W.; Gorecki, Chr. (ed.): Proc. SPIE Vol. 7064_2 (2008) - Interferometry XIV: Applications

[2] T. Luhmann, S. Robson, S. Kyle, I. Harley: Close Range Photogrammetry: Principles, Methods and Applications, revised edition 2011, Whittles Publishing, Scotland, UK

[3] N. R. Doloca: Random phase shift interferometer, Shaker Verlag Aachen 2008, Germany